

Design optimization and dynamic analysis of a tensegrity-based footbridge

Nizar Bel Hadj Ali*, Landolf Rhode-Barbarigos, Alberto Pascual Albi and Ian F.C. Smith

Applied Computing and Mechanics Laboratory
Ecole Polytechnique Fédérale de Lausanne (EPFL)
ENAC/IIC/IMAC, Station 18, 1015 Lausanne, Switzerland

Abstract

Tensegrity structures are spatial structural systems composed of struts and cables with pin-jointed connections. Their stability is provided by the self-stress state in tensioned and compressed members. Although much progress has been made in advancing research into the tensegrity concept, a rapid survey of current activities in engineering practice shows that much of its potential has yet to be accomplished. A design optimization study for a tensegrity-based footbridge is presented in order to further advance the tensegrity concept in modern structural engineering. In the absence of specific design guidelines, design requirements for a tensegrity footbridge are stated. A genetic algorithm based optimization scheme is used to find a cost-effective design solution. The dynamic performance of the tensegrity footbridge is studied through parametric studies. Design results illustrate that the proposed tensegrity-based footbridge meets typical static and dynamic design criteria.

Keywords:

Tensegrity structures, Design optimization, Footbridge design, Dynamic behavior, Genetic algorithm

1. Introduction

Tensegrity structures are spatial structural systems composed of struts and cables. They belong to a class of free-standing pin-jointed structures where stability is provided by the self-stress state in tensioned and compressed elements. A widely accepted definition has been proposed by Motro [1]: "*A tensegrity is a system in stable self-equilibrated state comprising a discontinuous set of compressed components inside a continuum of tensioned components*". This definition includes systems where compressed elements are interconnected as tensegrity structures. The tensegrity concept has received significant interest among scientists and engineers throughout disciplines such as architecture, civil engineering, biology, robotics and aerospace engineering [2]. While the concept is over 50 years old, a survey of current activities in research and engineering practice shows that much of its potential has yet to be accomplished.

Amongst civil engineering applications, the tensegrity concept can provide a rich opportunity for engineers and architects to explore new ideas and produce original structural forms. Tensegrity systems present attractive inspiration for structural expression in civil engineering offering elegant appearance together with high strength-to-weight ratios. Although free-standing tensegrity systems with discontinuous struts are not lightweight comparing to conventional civil engineering structures, continuous strut configurations present high structural efficiency [3, 4]. Moreover, unlike cable nets, no reaction forces have to be anchored to the ground. There are, however, few large-scale examples of tensegrity structures. Among the rare tensegrity-based civil structures that have been built, there is the tensegrity platform designed by Parnesso and Passera for the 2002 Swiss National Exhibition in Yverdon [5]. Parnesso and Passera also designed a tensegrity roof for a velodrome in Aigle (Switzerland) [6]. The Rostock tower (Germany), designed by Schlaich, Bergermann and Partners is composed of a continuous assembly of simplex modules. The Rostock tower, built in 2003, is the tallest tensegrity-based construction (62.3 m) [7, 8]. Large scale laboratory prototypes also exist. Fest et al. [9] built a 15m² double layer tensegrity prototype. The structure is used to explore the potential of active tensegrities [10-12]. A tensegrity grid covering a 82m² area was built at LMGC (Montpellier) [13]. This double-layer steel structure weighing 900kg has been designed according to the Eurocode3 building standard. Recently, the Kurilpa Bridge in Brisbane (Australia) became the largest tensegrity-inspired bridge in the world. The pedestrian and cycle bridge is designed by Cox Rayner Architects and Arup. The bridge is 470m long with a main span of 120m. Even though the Kurilpa Bridge is not strictly classified as a tensegrity structure, this project showed effectiveness and buildability of tensegrity-inspired civil engineering structures.

In spite of much research related to geometry, form-finding and architecture of tensegrity structures, few studies have focused on design and optimization of tensegrity-based civil structures. Motro and Hanaor initiated design studies on double-layer tensegrity grids [14, 15]. Investigation into double-layer tensegrity design are also made by Quirant et al [16]. Abedi and Shekastehband [17] investigated stability behaviour of plane tensegrity structures. Micheletti [18, 19] proposed tensegrity modules for a 32m-span tensegrity footbridge to be constructed in TorVergata (Italy). Wang and Li published papers concerned with tensegrity grid design [3, 20, 21]. Jensen et al [22] designed a tensegrity structure for an offshore aquaculture installation and concluded that the tensegrity concept shows promising properties for such applications. Liapi [23] developed tensegrity configurations for the lightweight parts of the Hellenic Maritime museum in Greece. This study investigated geometric and structural design taking into account assembly and erection considerations. De Oliveira et al [24] analytically investigated minimum mass design of tensegrity towers and plates. Recently, Motro [25] proposed a new family of tensegrity modules called "tensegrity rings" that can be assembled in a "hollow rope". As shown in previous work [26, 27], the concept of "hollow rope" shows promise for architecture and civil engineering applications such as footbridges. Few studies on design and optimization of tensegrity structures have been observed to be of practical significance. Except for tensegrity plane grids, design studies are mainly

performed for small and simple modules. Optimized tensegrity structures are much simpler than would be needed for practical civil engineering applications.

Tensegrities are highly coupled structures that often experience large displacements and therefore analysis should include geometrical nonlinearity. The properties of low self-weight, flexibility and nonlinear response to load combine to form challenging tasks for engineers aiming to use the tensegrity concept in civil structures. Moreover, studies on simple tensegrity structures have revealed the importance of design parameters such as the level of self-stress and the stiffness ratio between tensioned and compressed members [28]. The self-stress is necessary for stabilizing the structure by activating the geometrical stiffness of the tensegrity members. It increases load-bearing capacity but may introduce difficulties during the manufacturing process. This suggests that the self-stress level should be taken into account as a design variable together with the cross-sectional areas of tensioned and compressed members [29]. Due to these peculiarities, design of tensegrity structures can be a complex task which suggests the use of design optimization techniques [16].

Structural optimization has been widely studied over the last decades and extensive work has been done in the area of optimal design of steel trusses and frames. Most of these studies focus on weight minimization since engineers have few tools to approach cost optimization in a systematic manner [30, 31]. However, designing tensegrity structures based on weight minimization is particularly inefficient. In addition to material cost, tensegrities require additional pretensioning labor and careful assembling on-site [32]. Consequently, this leads to higher labor costs compared with conventional spatial truss structures. A realistic design optimization of a tensegrity structure should thus be based on cost minimization rather than weight minimization. Although structural optimization has been studied extensively, no study has examined cost optimization of a tensegrity civil structure.

This paper presents design optimization and dynamic analysis of a tensegrity-based civil structure. A pentagonal hollow rope is used as a structural system for a 21m-span footbridge. The topology of the footbridge includes bar-to-bar connections, allowing for a lightweight solution. The footbridge design is optimized based on a novel approach where both structural members and self-stress levels are chosen for minimal cost. The footbridge is designed according to Swiss civil engineering building practice. Design optimization is conducted through a genetic algorithm (GA). The design algorithm finds solutions with minimum cost and also ensures that stresses and displacements are within the limits defined by the Swiss code. The footbridge members are sized using standard steel sections and stainless steel cables. A sensitivity analysis is performed to investigate the influence of design variables on optimization results. The dynamic behaviour of the tensegrity-based footbridge is also analyzed. Parametric studies are performed to identify parameters that significantly affect the dynamic characteristics of the tensegrity footbridge.

2. Tensegrity mechanics

Tensegrity systems can be regarded as a special class of spatial truss structures that are composed of struts and tendons. Tensioned and compressed components are assembled in a self-equilibrated system providing stability and stiffness to the structure.

The first step in the design of tensegrity structures is the determination of their equilibrium configuration. This step, known as form-finding, is the first challenge that engineers need to tackle when designing tensegrity structures. Tensegrity form-finding has received widespread attention over the years resulting in several methods such as nonlinear programming techniques [33], dynamic relaxation [34], force density [35] and stochastic search [36]. An exhaustive review of form-finding methods for tensegrities can be found in [37, 38].

Kinematic and static properties of a tensegrity structure can be investigated once a stable configuration is identified. Two major parameters are required for the characterization of a tensegrity structure: the number of self-stress states (s) and the number of mechanisms (m). These parameters determine the degree of static and kinematic indeterminacy of a tensegrity structure [4, 39]. Calladine [40] investigated the statics of tensegrity structures and showed that the structural parameters, (s) and (m), are related through an extended Maxwell's rule. For a three dimensional tensegrity framework, with N_m members connected in N_j joints and restrained by N_k displacement constraints, the set of equilibrium equations can be expressed as follow:

$$[A]\{t\} = \{F\} \quad [\text{Eq. 1}]$$

where $[A]$ is the equilibrium matrix consisting of element direction cosines, $\{t\}$ is the internal element force vector of length N_m and $\{F\}$ is the external nodal force vector of length $3N_j - N_k$. Assuming that the rank of the equilibrium matrix is r_A , the number of self-stress states and the number of mechanisms are given by:

$$s = N_m - r_A \quad [\text{Eq. 2}]$$

$$m = 3N_j - N_k - r_A \quad [\text{Eq. 3}]$$

The number of states of self-stress indicates the number of non-trivial solutions to the equilibrium equation (Eq. (1)) when: $\{F\} = \{0\}$. The basis of vector spaces of self-stress states and mechanisms are calculated from the null spaces of the equilibrium matrix [41]. A general self-stress configuration can be then obtained by any linear combination of the (s) independent self-stress states. It is noticed that the number (s) represents also the number of pretensioning devices which are needed to establish the general self-stress state in the structure. Moreover, for a tensegrity structure, cables have uniaxial tension behavior while bars experience generally compressive stresses. A tensegrity self-stressed configuration is said to be compatible if it ensures tension in cables and compression in bars.

3. Analysis of tensegrity structures

Tensegrity structures have a nonlinear mechanical behavior in response to external loading. Since tensegrities are self-stressed, the effects of the changing geometry on the orientation of already stressed elements must be taken into account [42]. Nonlinear models and iterative computational schemes are then needed for the static analysis of tensegrity structures. In this context, two basic approaches have been developed and applied in practice. The first one is a standard nonlinear structural analysis scheme where the static equilibrium equation is solved incrementally using modified Newton-Raphson procedure [28]. The second is dynamic relaxation: an iterative procedure which was first introduced by Day [43] and has been reliably applied to tensile structures [34], tensegrities and many other nonlinear problems. In this method, a fictitious dynamic model is used to trace the motion of a structure from the time of loading to the moment when static equilibrium is attained due to damping [34].

In a linearized form of the equilibrium equation of a tensegrity system, displacement vector $\{U\}$ and external force vector $\{F\}$ are related by the tangent stiffness matrix $[K_T]$,

$$[K_T]\{U\} = \{F\} \quad [\text{Eq. 4}]$$

In the literature there are several methods to derive the geometrical stiffness matrix of tensegrity structures [28, 44-46]. According to the formulation presented by Kebiche et al [28], the tangent stiffness matrix is written as:

$$[K_T] = [K_E] + [K_G] \quad [\text{Eq. 5}]$$

The tangent stiffness matrix $[K_T]$ is decomposed into the linear stiffness matrix $[K_E]$, commonly used for small-deformation truss analyses, and the geometrical stiffness matrix $[K_G]$, induced by self-stresses. For the development of a finite element model of the tensegrity structure, each element in the structure is characterized by the following stiffness matrices:

$$[K_E] = \left(\frac{EA}{L}\right) \begin{bmatrix} I_0 & -I_0 \\ -I_0 & I_0 \end{bmatrix}; I_0 = \begin{bmatrix} 1 & 0 & 0 \\ 0 & 0 & 0 \\ 0 & 0 & 0 \end{bmatrix} \quad [\text{Eq. 6}]$$

$$[K_G] = \left(\frac{T}{L}\right) \begin{bmatrix} I_3 & -I_3 \\ -I_3 & I_3 \end{bmatrix}; I_3 = \begin{bmatrix} 1 & 0 & 0 \\ 0 & 1 & 0 \\ 0 & 0 & 1 \end{bmatrix} \quad [\text{Eq. 7}]$$

where: E is the elastic modulus, A is the member area, L is the length of the member and T is the internal axial force. Stiffness matrices are first formulated in a local coordinate system $\{xyz\}$ where x is along the element axis. The global stiffness matrix $[K_T]$ is

obtained by adding up contributions from the individual elements expressed in a global coordinate system. Static analysis of tensegrity structures can thus be performed iteratively using transient stiffness method [28].

4. Design requirements of a tensegrity-based footbridge

In the absence of specific codes, design requirements for footbridges are gathered from numerous documents, guidelines and recommendations [47]. This situation has partially changed following the opening events of the London Millennium Bridge. These events have motivated research into static and dynamic behaviour of footbridges and have contributed to significant progress in footbridge design. Consequently, codes for footbridges are presently available in several countries [48, 49].

In terms of geometry specifications, the Swiss code does not give information about minimum deck width, clearance and maximum inclination. The British Standard recommends a minimum deck width of 2m in case of non-motorized traffic (pedestrian and cyclists) [50]. A minimum clearance of about 2.3m is required in [49].

Different live load values are specified in national codes. The Swiss code SIA 261 [51] proposes two models: a distributed load of 4kN/m^2 and a point load of 10kN. The most critical among the two live load models is considered for design activities. Together with vertical loads, a second load acting in the axis of the carriageway is considered. The horizontal force value corresponds to 10% of the sum of the uniformly distributed load or 60% of the concentrated load. Snow loading is unlikely to be significant when the bridge is being heavily used. Consequently, the SIA 260 code [52] states that snow loads are only to be considered as an accompanying action for covered bridges. Vertical design loads for footbridges include also dead loading that represents the distributed weight of the footbridge superstructure including decking.

Wind loading is also to be considered in footbridge design. Wind loading, acting on the exposed side faces of the bridge members, is calculated considering a uniform wind pressure of 130 to 140 daN/m^2 . Wind loading is usually considered as accompanying action and hence assigned a reduction factor in load combinations [52].

A tensegrity-based footbridge has to be designed to meet usual norms for safety and serviceability. However, regarding the peculiarity of tensegrities as self-stressed systems, two additional aspects have to be considered. First, the unidirectional behaviour of tensioned elements in a tensegrity structure imposes to take into consideration an additional criterion intended to prevent the presence of slack cables in the structure under service loads. This restriction is not only justified by esthetic aspects but also by the fact that slack cables can cause shocks and create disturbances when they repeatedly pass from a slack state to a tensioned state and vice-versa [16]. Moreover, it must be emphasized that self-stresses play a double role in a tensegrity structure and can be regarded as acting differently when structural overall stability or member local resistance are concerned. In fact, the self-stress can be considered as a stabilizing load when the

overall stability of the structure is verified. However, it must be considered as a destabilizing load, and thus assigned a bigger load factor, for member local capacity checks.

Considering the above mentioned design aspects proper to tensegrity structures, two load combinations will be considered for Ultimate Limit State (ULS) verifications. In Eq. (8) and (9), dead load (G), live load (Q), wind load (W) and loads due to self-stress (P) are combined differently depending on whether the combination is employed to verify the overall stability of the structure or the local member resistance. In the absence of definite information in civil engineering codes, the self-stress will be assigned a load factor of 0.8 (1.2, respectively) when it is considered to act as a stabilizing load (unstabilizing load, respectively). These values were proposed by Quirant et al [16] for the design of a double layer tensegrity grid.

$$1.35G + 1.5Q + 0.8P + 0.6W \quad [\text{Eq. 8}]$$

$$1.35G + 1.5Q + 1.2P + 0.6W \quad [\text{Eq. 9}]$$

The first ULS load combination (Eq. (8)) is used to verify overall stability of the tensegrity structure. The second load combination (Eq. (9)) is used for local capacity and buckling checks.

Under Serviceability Limit States (SLS), design loads are combined as follow:

$$1.0G + 0.4Q + 1.0P + 0.6W \quad [\text{Eq. 10}]$$

Serviceability design criteria include limiting deformations and vibrations that impair the functionality or appearance of the structure. As specified by SIA 260 [52], the maximum midspan deflection of the footbridge is limited to $\text{Span}/600$.

Amongst structural concerns, dynamics of tensegrity-based footbridges is a central issue. A careful evaluation is required when using these lightweight structural systems for footbridges to avoid excessive dynamic response. Tensegrity structures have relatively low inherent structural damping. This factor coupled with the low self-weight may cause tensegrity footbridges to experience unacceptable vibration levels in response to pedestrian and/or wind loads. For dynamic behaviour, acceptance criteria defined by the Swiss codes are frequency-dependent. In the vertical direction, natural frequencies of footbridges in the range of 1.6 Hz to 4.5 Hz must be avoided. In the horizontal direction, natural frequencies smaller than 1.3 Hz and 2.5 Hz must be avoided for transverse and longitudinal vibrations respectively.

5. Design optimization problem

5.1 Objective function

A realistic design optimization of a tensegrity structure should be based on cost optimization. In the absence of definite information about fabrication and assembling activities for tensegrity structures, we propose a simplified cost function calculated as the sum of material member costs multiplied by a coefficient depending on the self stress level (Eq. (11)).

$$\text{Min } C = (1 + \psi) \sum_{i=1}^{N_m} c_i L_i \quad [\text{Eq. 11}]$$

In the objective function (Eq. (11)), the sum of member material costs of a design solution is increased proportionally to the self-stress ratio in the tensegrity structure. The self-stress ratio ψ is calculated as the average self-stress ratio considered for tensioned elements. For a tensioned member, the self-stress ratio is calculated as the ratio between the member pretension axial force and its resistance axial force. It should be pointed out that tensioning devices are needed only for (s) members, where (s) is the number of independent self-stress states of the structure. In Eq. (11), L_i is the length of member i , and c_i is the cost per unit length of the section that is assigned to member i . N_m is the total number of tensegrity members. It should be pointed out that the most important factor affecting the total cost of the tensegrity structure is potentially the cost of the joints. In steel construction joints are very expensive details that may determine other aspects of the design of a structure [30]. In this study, only a single topology is analyzed. Therefore, the number of joints and hence, the cost of joints is assumed to remain constant for all design solutions.

5.2 Design constraints

The design constraints (Eq. 12 to 15) are formulated according to SIA codes [53]. In these equations N_{cm} and N_{tm} are the numbers of compressed and tensioned members in the structure.

$$\frac{N_{sd,i}}{N_{Rd,i}} - 1 \leq 0, \quad i = 1, \dots, N_m \quad [\text{Eq. 12}]$$

$$\frac{\lambda_i}{\lambda_{k,i}} - 1 \leq 0, \quad i = 1, \dots, N_{cm} \quad [\text{Eq. 13}]$$

$$\frac{\delta_{midspan}}{\delta_{limit}} - 1 \leq 0 \quad [\text{Eq. 14}]$$

$$N_{sd,i} > 0, \quad i = 1, \dots, N_m \quad [\text{Eq. 15}]$$

Eq. (12) defines the local capacity and buckling checks for tensioned and compressed members. $N_{sd,i}$ is the ultimate axial force of member i , while $N_{Rd,i}$ is its axial force resistance. For tensioned members, the resistance is calculated using Eq. (16) where f_y is the yield stress of the steel and A is the cross-sectional area of the member.

$$N_{Rd} = \frac{f_y A}{1.05} \quad [\text{Eq. 16}]$$

For compressed members $N_{Rd,i}$ is determined as the buckling force limit (Eq.17) in which χ_k is a reduction factor for buckling.

$$N_{k,Rd} = \chi_k f_y A / 1.05 \quad [\text{Eq. 17}]$$

The slenderness limit (Eq. 13) for compressed elements prevents local instability for strut members. The maximum slenderness shall not exceed a value of 200. Eq. (14) and (15) define the serviceability limit state requirements for the tensegrity footbridge.

5.3 Design variables

From a structural point of view, tensegrity structures are characterized by the self-stress state that ensures their stability. Self-stress is necessary for stabilizing the structure by activating the geometrical stiffness. The equilibrium between tension and compression forces is responsible for the structural stability and load bearing capacity of tensegrities. Previous studies have found that the self-stress level initially introduced in tensegrity members before applying loads have a direct impact on both the weight and the deflection of the tensegrity footbridge [26, 27]. This suggests that initial self-stresses, together with the cross-sectional areas of tensioned and compressed members are the key design parameters that affect the structural performance and cost of a tensegrity structure.

6. Static design of a tensegrity-based footbridge

6.1 Structure description

A side view of the tensegrity based footbridge is given in Fig. 1. The footbridge is composed of six ring-shaped tensegrity modules connected base to base to span 21.6m (Figure 1). Symmetry about midspan is obtained by mirroring three modules. The structure is designed so that to have 2.0m width internal space for walking and a clearance of 2.5m as recommended by codes [50]. The dimensions of the free space are conceived so as to have enough room for non-motorized traffic (pedestrian and cyclists). The nodes of the footbridge structure at both extremities are supposed to be attached to a steel frame which is rigidly anchored to the ground. The footbridge deck is connected to

four base nodes at each module and it is supposed that the deck does not increase the number of independent self-stress states.

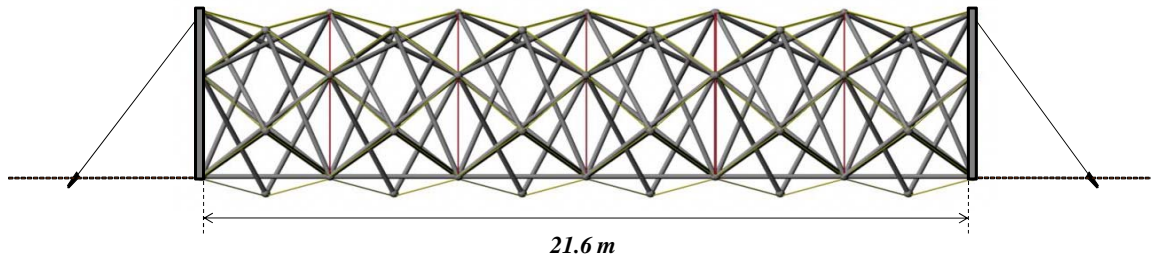


Figure 1. The tensegrity footbridge

The tensegrity module is a continuous ring module with a single strut circuit. This tensegrity module is called a pentagon module [25, 27]. A pentagon module contains 15 nodes describing 3 pentagonal layers (Figure 2). The middle pentagonal layer nodes are rotated about the longitudinal axes with respect to outer pentagon by 36° in the counterclockwise direction. The pentagon module comprises 15 struts held together in space by 30 cables forming a ring shaped tensegrity unit. Struts can be separated into diagonal and intermediate struts based on their topology. Diagonal struts connect outer and inner pentagon nodes while intermediate struts connect middle pentagon nodes to outer and inner pentagon nodes. Similarly, cables are separated into 10 layer cables and 20 x-cables. Layer cables connect nodes of the two outer pentagons while x-cables connect middle pentagon nodes to inner and outer pentagon nodes (Figure 3). In Figures 1 to 3, grayed lines denote bars while thin lines denote cables.

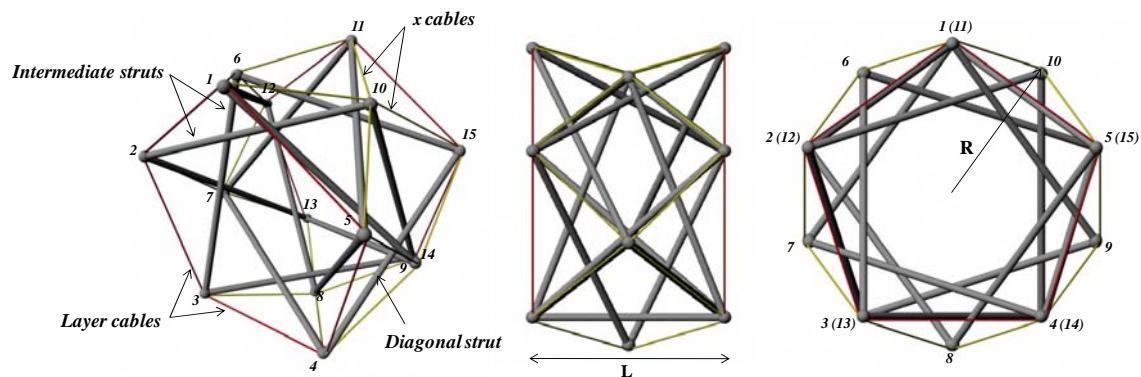


Figure 2. The pentagon module

The pentagon module used in this study has a length of 360cm with an inner radius of 280cm. This geometry satisfies internal space requirements. Diagonal and intermediate struts are chosen to have the same length of 488cm. Layer cables have a length of 330cm while x-cables are 250cm length. The nodes of the structure at both extremities are supposed to be fixed in all three translation directions. Live loads are applied on the footbridge deck and are thus transmitted to the four bottom nodes on each module. Dead and wind loads are also applied as nodal forces on the structure.

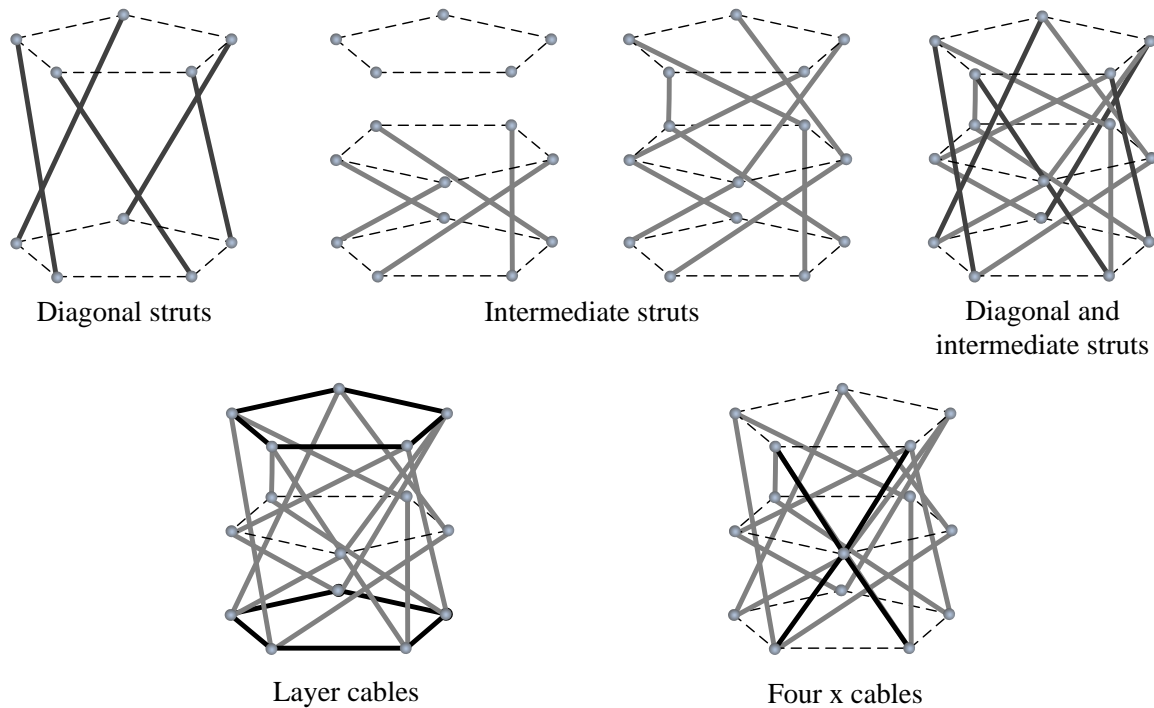


Figure 3. Illustration of the pentagon module members

Prior to footbridge design optimization, mechanical characterization of the basic pentagon module and the whole structure of the footbridge are performed. The study of the equilibrium matrix of the two structures is performed considering 6 blocked degrees of freedom to prevent rigid body movements. The footbridge is also analyzed when nodes at both extremities are fully constrained. The results illustrated in Table 1 reveal the existence of 6 elementary self-stress states for the pentagon module and 56 self-stress states for the footbridge while no infinitesimal mechanisms are detected. The footbridge structure has 80 self-stress states when all nodes at both extremities are constrained. The pentagon module and the tensegrity footbridge are thus statically indeterminate but kinetically determinate structures. The absence of infinitesimal mechanisms in the tensegrity footbridge affects the structural efficiency and the dynamic behaviour of the footbridge as will be shown in forthcoming sections.

Table 1. Mechanics parameters for the tensegrity-based module and footbridge			
Parameter	Pentagon module	Pentagon footbridge	Pentagon footbridge (fully constrained)
Rank of equilibrium matrix	39	189	165
Number of mechanisms: m	0	0	0
Number of self-stress states: s	6	56	80

6.2 Design optimization

Design optimization of the tensegrity-based footbridge is performed using member dimensions and self-stress level as design variables. Struts are separated into two design groups: diagonal and intermediate struts. Strut members in each group are to have the same hollow tube section profile. Layer cables in the whole footbridge are specified to be of same section and experience the same level of self-stress. The same hypothesis is taken into account for x-cables. Optimization variables are thus limited to 6 groups: cross-sectional sizes of diagonal struts, intermediate struts, layer cables and x-cables in addition to self-stress ratios for layer cables and x-cables.

The footbridge members are selected from commercially available standard steel sections with specified cross-sectional profiles and cables. For struts, the product set consists of 45 hollow tube section profiles. The cross-section dimensions, properties and unit prices of these profiles are listed in Table A.1 (Appendix A). The used steel grade is S355, with a modulus of elasticity of 210000 MPa and yield stress of 355 MPa. For cables, a list of 22 sections is used. Cable properties and unit prices are listed in Table A.2 (Appendix A). Cables are made by stainless steel with a modulus of elasticity of 120000 MPa. Material properties and unit prices are obtained from major Swiss steel fabricators. Design variables include also the self-stress level in the tensegrity structure. Nine discrete self-stress ratios are considered running between zero and 20% by steps of 2.5%. The prestress is established in tensegrity members by changing their rest lengths. It should be pointed out that the final member stresses, after taking into account the self-weight of the structure, are different from the initially prescribed prestresses.

Load cases defined in section 2.3 are considered. The footbridge deck is assumed to have a weight of 100kg/m^2 . Structural analyses for load combinations are performed using a MATLAB[®] implementation of nonlinear analysis employing transient stiffness method. Analysis results are used to check the footbridge design constraints.

A GA is employed to solve the design optimization task (Eq. 11 to 15). Optimization variables are coded as integer strings. Penalty functions are employed to handle design constraints. This consists on penalizing individuals violating constraints, and thus giving them a lower probability of survival. The penalty function approach is implemented by adding an additional term to the objective function. This additional term corresponds to the cost of violating constraints. In this manner, the search for optimum solutions is directed towards feasible regions of the search space.

Optimization results are quite satisfactory for a population size of 50 individuals running for 60 generations. Crossover and mutation probabilities are fixed as 0.9 and 0.1, respectively. The best solution generated over a sequence of five runs using different random seeds is considered as the optimal design solution.

Table 2. Member sections and self-stress ratios of the optimal design solution

Member	Diameter [mm]	Cross-sectional area [mm ²]	Self-stress ratio [%]
Diagonal struts	76.1	902.0	-
Intermediate struts	101.6	1230.0	-
Layer cables	6	28.27	15.0
x-cables	20	314.16	17.5

The optimal design attained after five runs of the GA has a material cost of 41622.0 CHF and a cost function value of 48386.0 CHF. The member sections and self-stress ratios for the design solution are displayed in Table 2. Under SLS load combination, midspan displacement for the design solution is equal to 2.37cm. Under ULS load combinations, a maximum axial compression of 102.0kN is obtained in intermediate struts which represent 96% of their buckling capacity. Diagonal struts are less stressed with a maximum compression load of 39.5kN representing 88% of their buckling capacity. Maximum tension forces of 162kN and 13.5kN are obtained for x-cables and layer cables respectively. Tension forces in x-cable and layer cables represent 48.2% and 44.7% of their respective tension capacities.

6.3 Sensitivity analysis of the designed solution

A sensitivity analysis is conducted in order to determine the influence of the self-stress level on the cost of the footbridge design solutions. The evolution of the optimal design cost is thus studied with respect to the self-stress level. Self-stress ratios in layer cables and x-cables are varied from 5% to 20% in steps of 2.5% and for each value, a GA is employed to search for minimum cost design. Design optimization is thus performed considering only the member cross-section sizes as design variables. Variation of optimal design cost with respect to self-stress ratios in layer and x-cables is illustrated in Figure 4. It can be seen that small self-stress levels lead to higher costs. The optimal design cost of the footbridge is almost constant for values of self-stress ratios between 12.5% and 20%. Optimization results show also that the optimal solution obtained with 20% self-stress ratio for the two sets of cables has a cost of 49479 CHF. This solution is 2% more expensive compared to the best design solution obtained with a smaller level of self-stress (15% in layer cables and 17.5% in x-cables). This suggests that increasing self-stress level beyond certain limits may not lead to better solutions.

When the self-stress ratio is not taken into account in the objective function, optimization results show that the material cost can be reduced by increasing the self-stress level. The minimum material cost is thus obtained with the highest self-stress level in the tensegrity footbridge (20%). In spite of this development, it is recognized that the major cost of this structure will come from fabrication of the joints. Recall that in this study it is assumed that the number of joints is fixed and that their cost is independent of the level of self-stress and element sizes.

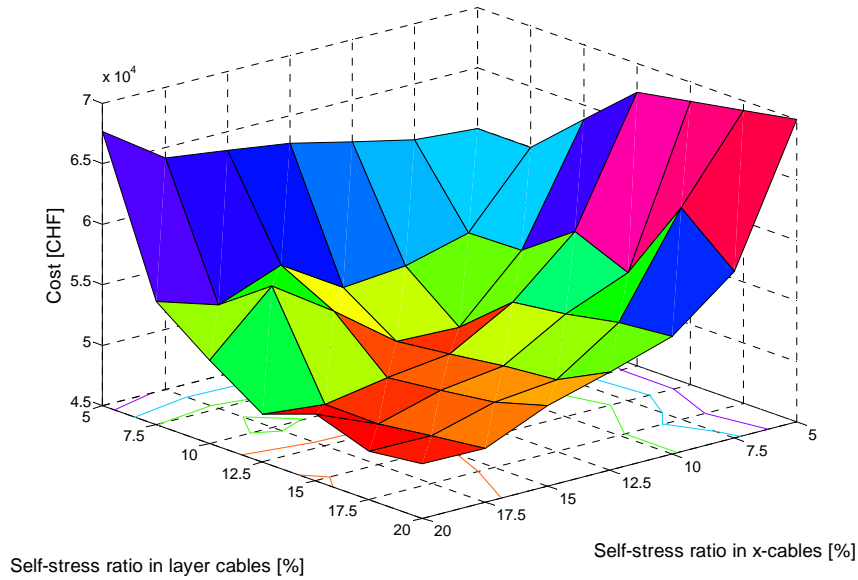


Figure 4. Variation of optimal design cost with respect to self-stress ratios in layer and x-cables

7. Dynamic behaviour of the tensegrity footbridge

7.1 Eigenfrequency analysis

The linearized equation of motion of a tensegrity structure at a defined self-stressed configuration can be expressed as follow:

$$[M]\{\ddot{u}\} + [K_T]\{u\} = \{F\} \quad [\text{Eq. 18}]$$

where: $[M]$ and $[K_T]$ are mass and tangent stiffness matrices, respectively. $\{F\}$ is the applied load vector. u , and \ddot{u} are respectively vectors of nodal displacement and acceleration. The standard eigenproblem expressed in Eq. (19) is obtained from Eq. (18) for a small harmonic motion of the form: $\{u\} = \{\bar{u}\} \sin(\omega t)$, where ω is the angular frequency and $\{\bar{u}\}$ is the displacement amplitude vector.

$$[K_T]\{\bar{u}\} = \omega^2 [M]\{\bar{u}\} \quad [\text{Eq. 19}]$$

The spectral decomposition of matrix $[M^{-1}K_T]$ yields the natural frequencies and corresponding mode shapes of the tensegrity footbridge.

Eigenfrequency analysis is first performed for the design solution obtained in section 6.2. The mass of the footbridge deck is taken into account in the mass matrix. Natural frequencies are presented for the five lowest modes in Hz (Table 3).

Table 3. Natural frequencies of the tensegrity footbridge

Mode	Mode type	Natural frequency (Hz)
1 st mode	Lateral bending	6.00
2 nd mode	Vertical bending	6.05
3 rd mode	Torsion	11.76
4 th mode	Lateral bending	13.75
5 th mode	Vertical bending	13.83

Eigenfrequency analysis results show the existence of pairs of modes with close frequencies. The first and second modes correspond to the first and second bending modes of a simply supported beam. The third mode is a torsion mode. The fourth and fifth modes have very close frequencies and correspond to lateral and vertical bending modes with two half waves. Modes corresponding to the first five natural frequencies are all identified as deformation modes. The absence of soft modes usually detected in tensegrity structures is due to the fact that the tensegrity footbridge has no infinitesimal mechanisms as shown by the mechanical characterization (Table 1).

It should be pointed out that pedestrian mass is comparable with that of the footbridge and thus could alter the vibration frequencies. The evolution of the five first natural frequencies is studied with respect to the number of pedestrians per m^2 of the footbridge deck. In this case pedestrian mass is taken into account in the mass matrix of the structure. Results illustrated in Fig. 5 show that the first natural frequencies decrease when the number of pedestrians on the footbridge increases. When the footbridge is not fully loaded (less than 2 pedestrians/ m^2), the first natural frequencies of the tensegrity footbridge meet acceptance criteria defined by the Swiss code in terms of dynamic behavior. The frequency of the first mode of vibration is not in the frequency range to be avoided. Recall that the live load to be taken into account in serviceability limit states correspond approximately to the weight of two pedestrians/ m^2 on the footbridge deck. Figure 5 also shows that when the footbridge is fully loaded (4 pedestrians/ m^2), the fundamental vibration frequency is below 4 Hz. This suggests that the footbridge should be rigorously studied under dynamic excitations induced by pedestrians.

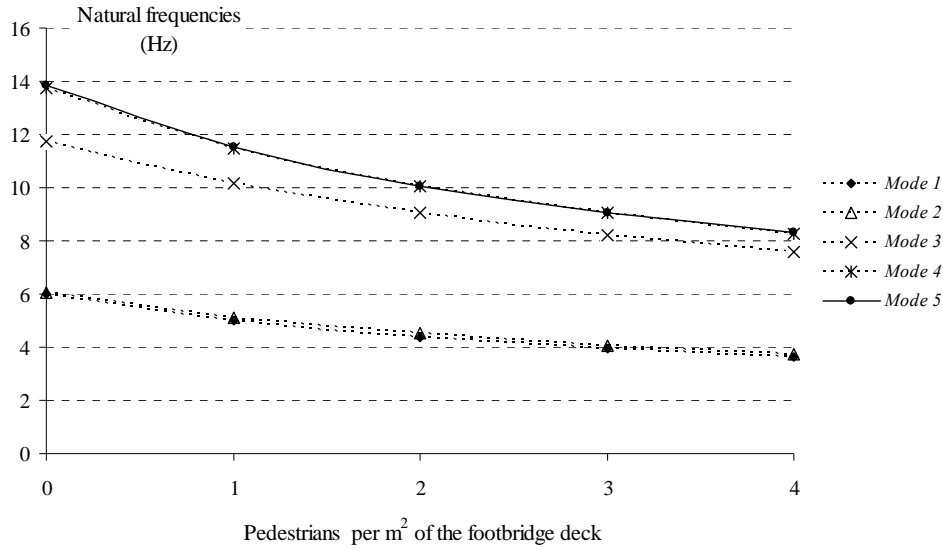


Figure 5. Variation of the natural frequencies with respect to the number of pedestrians on the footbridge

Table 4. Natural frequencies of the tensegrity footbridge for various self-stress levels

Mode	Self-stress ratio		
	5%	10%	20%
1 st Mode [Hz]	5.94	5.96	6.00
2 nd mode [Hz]	6.00	6.02	6.06
3 rd mode [Hz]	11.74	11.75	11.77
4 th mode [Hz]	13.61	13.66	13.78
5 th mode [Hz]	13.68	13.74	13.85

The evolution of the five first natural frequencies is also studied with respect to the self-stress level in the tensegrity footbridge. Eigenfrequency analysis is conducted with a self-stress ratio varying from 5% to 20%. The cross-sectional sizes for struts and cables are those obtained in section 6.2 while the same self-stress ratio is considered for layer and x-cables. Natural frequencies for first five modes for increasing self-stress levels are displayed in Table 4. Eigenfrequency analysis results show that the natural frequencies of the first five modes remain almost constant when the self-stress level is increased in the studied range. These results can be explained referring to the stiffness components of a tensegrity structure. As shown in Eq. (5), the tangent stiffness $[K_T]$ of a tensegrity structure is constituted by the elastic stiffness $[K_E]$, employed for small deformations truss analyses, and the geometrical stiffness $[K_G]$, induced by self-stresses. Consequently, when the structure experiences deformation modes, which have non-zero elastic energy, the stiffness is of the order of Young's modulus and hence slightly affected by increasing the degree of self-stress. However, for infinitesimal mechanism modes, the elastic term vanishes and the stiffness is then induced only by $[K_G]$ [12]. This shows that, for the tensegrity footbridge, the fundamental frequency cannot be modified by changing the self-stress level.

To further investigate the dynamic behavior of the design solutions obtained with various levels of self-stress, the first natural frequencies of the optimized designs are plotted with respect to the self-stress ratios in footbridge members (Figure 6). For the studied design solutions, the fundamental frequency ranges between 5 and 9Hz. The smallest frequency value is obtained with the highest level of self-stress in the structure. Since frequencies are not directly affected by the level of self-stress, this result is explained by a reduced structural mass due to high level of self-stress. In fact, design optimization with the highest level of self-stress (20%) result in 11% mass reduction compared to the design solution obtained with a self stress ratio of 5%.

Results illustrated in Fig. 6 show that it is possible to consider the dynamic behavior as additional parameter in the design process of the tensegrity footbridge. A final design solution can be chosen from a set of optimized designs with respect to its modal characteristics. The design optimization task of a tensegrity footbridge can be treated as a multi-objective task and techniques for Multi-Criteria Decision Making (MCDA) can be used to identify good design solutions.

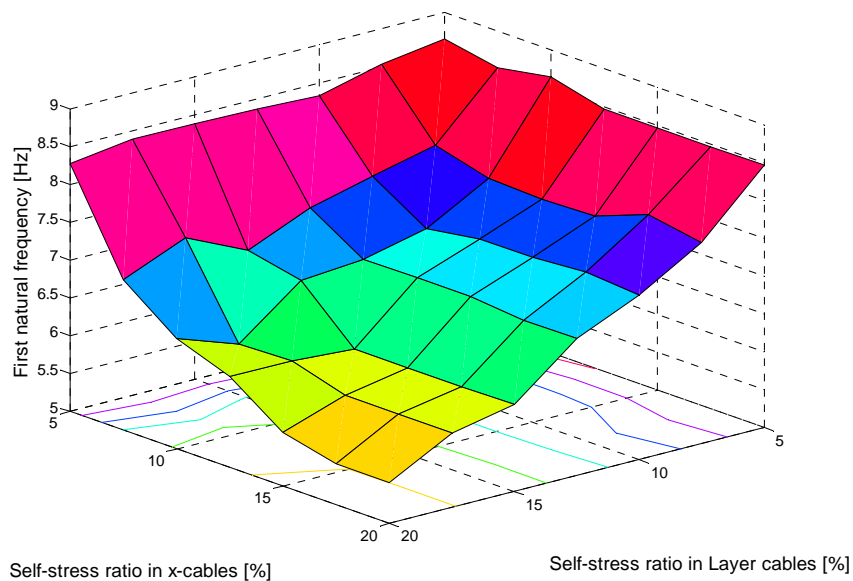


Figure 6. Variation of first natural frequency with respect to self-stress ratios in layer and x-cables

7.2 Parametric studies

To investigate the influence of design variables on the footbridge modal characteristics, parametric studies of element cross-sectional sizes versus natural frequencies are conducted. Four parameters are examined: the cross-sectional area of diagonal struts, intermediate struts, layer cables and finally x-cables. For each parameter, a range of values is studied while other parameters are left unchanged. The analysis thus reveals the

influence of each parameter assuming mutual independence. The design solution obtained in section 6.2 is considered as default configuration for each parametric study.

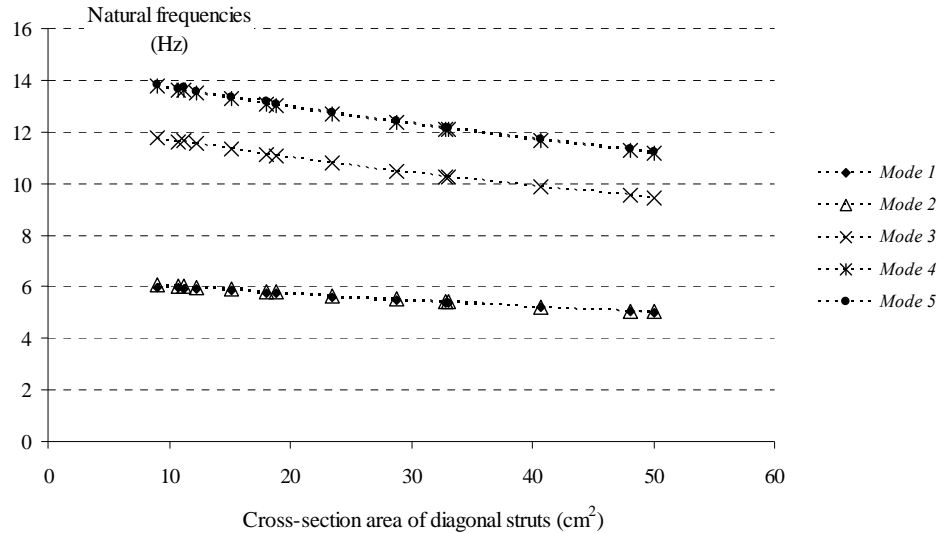


Figure 7. Variation of the natural frequencies with respect to the cross-section area of diagonal struts

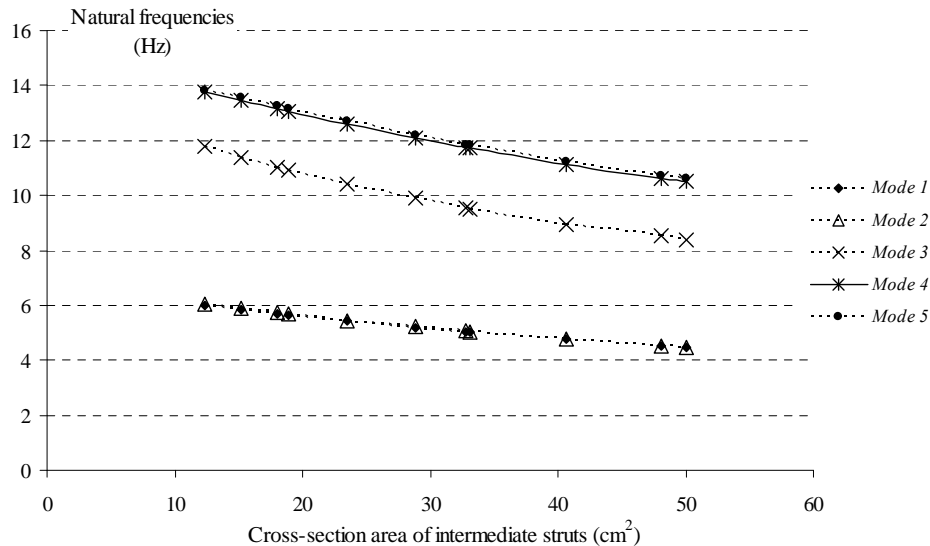


Figure 8. Variation of the natural frequencies with respect to the cross-section area of intermediate struts

The evolution of the first five natural frequencies with respect to the cross-sectional area of struts is illustrated in Fig. 7 for diagonal struts and Fig. 8 for intermediate struts. Values for cross-sectional areas are chosen from the list of standard hollow tube profiles (Appendix A – Table A1). Results illustrated in Figures 7 and 8 show that the footbridge natural frequencies decrease when the cross-sectional areas of struts are increased. This suggests that the increase in the stiffness of the footbridge is counter-balanced by a higher increase in structural mass leading the natural frequencies to decrease. An observation

emerging from the comparison between results illustrated in Figures 7 and 8 is that natural frequencies are influenced slightly more by cross-sectional area of intermediate struts than by diagonal strut cross-sectional area. This can be explained by the fact that the number of intermediate struts in the footbridge is more than twice the number of diagonal struts.

To further investigate the influence of cross-sectional parameters on modal characteristics of the tensegrity footbridge, the influence of changing cross-sectional areas of layer cables and x-cables is studied. Cable cross-sectional areas are chosen from a list of commercially available stainless-steel cables (Appendix A – Table A2).

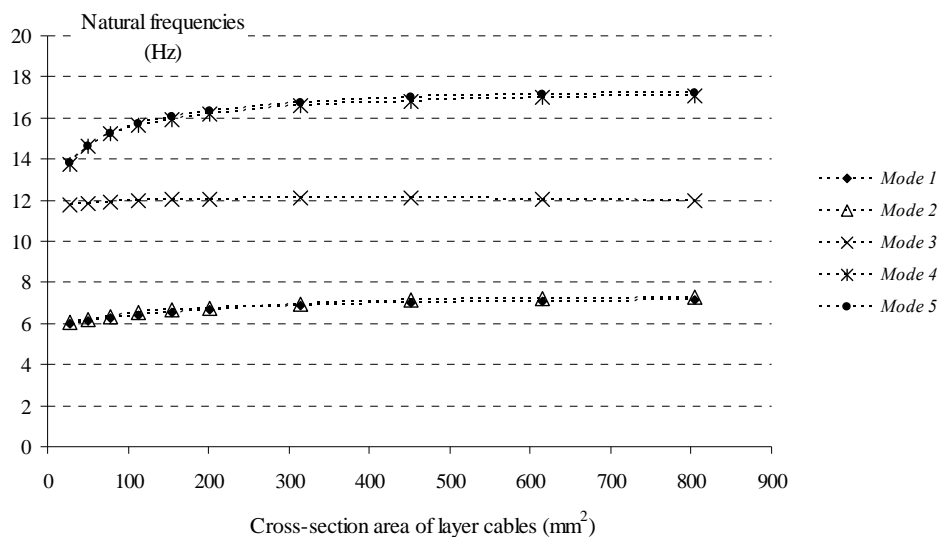


Figure 9. Variation of the natural frequencies with respect to the cross-section area of layer cables

The evolution of the first natural frequencies with respect to the cross-sectional area of layer cables is illustrated in Fig. 9. It can be seen from this figure that the first natural frequencies of the footbridge increase when the cross-sectional area of layer cable is increased. Similarly, as shown in Fig. 10, natural frequencies can be increased by increasing the cross-sectional area of x-cables. Results illustrated in this figure show an expected trend. In fact, an increment of the cross-sectional area of x-cables results in an increased stiffness of the structures without significantly increasing dead loads. This is also the case for layer cables in a minor degree. It is observed that natural frequencies are more influenced by change in x-cable cross-sectional area compared to change in layer cables. This suggests that the stiffness of the tensegrity footbridge is more influenced by cross-sectional characteristics of x-cables.

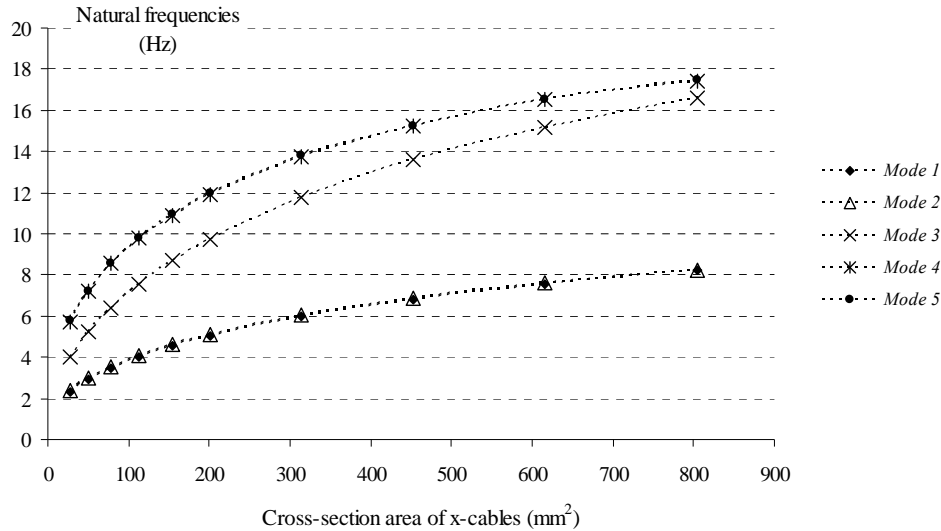


Figure 10. Variation of the natural frequencies with respect to the cross-section area of x-cables

8. Conclusions

The tensegrity concept presents new opportunities for structural expression in civil engineering offering safety and serviceability together with an elegant appearance and high strength-to-weight ratio. Although, tensegrities have been around for fifty years, tensegrity systems are not yet recognized as feasible engineering solutions. In this paper, the feasibility of using the tensegrity concept in a footbridge structural system is investigated through design optimization and a dynamic study. A GA is employed to find minimal cost design solutions. Design constraints are formulated according to the Swiss code of practice.

The following conclusions come out from this study:

- High flexibility hindered the use of tensegrity systems in civil structures. However, this study showed that tensegrity systems with connected compression elements could compete with traditional structural systems. Based on a ring module topology, a minimum-cost design solution satisfying all footbridge design requirements is identified.
- The sensitivity analysis showed the importance of the level of self-stress as a design parameter. Design solutions obtained through material cost minimization have relatively high self-stress level which increases labor costs. This justifies explicitly taking into account self-stress costs in order to ensure a consistent design optimization of the tensegrity-based footbridge.
- Eigenfrequency analysis results showed that the fundamental frequency of the tensegrity footbridge is not directly influenced by the self-stress level. However, results of parametric studies showed that natural frequencies are influenced by

other design parameters such as the cross-sectional sizes of x-cables. It is thus possible to consider the dynamic behavior as additional parameter in the design process of the tensegrity footbridge.

- Although tensegrity structures are lightweight and have relatively low inherent structural damping, eigenfrequency analysis results showed that the tensegrity-based footbridge can withstand dynamic loads such as those induced by a small number of pedestrians.

These results underline the complexity of the design of tensegrity structures and the need for advanced computing methods. The design optimization study of a tensegrity-based footbridge is aimed to be a novel contribution toward identifying potential application of the tensegrity concept in civil structures.

Acknowledgements

The authors would like to thank the Swiss National Science Foundation for supporting this work (FN Grant no 200020-121552/1). Prof. René Motro and Dr. Prakash Kripakaran are thanked for discussion and advice.

Appendix A.

Table A.1 Hollow tube profile properties

N°	External diameter [mm]	Thickness [mm]	Cross-sectional area [cm ²]	Moment of inertia [cm ⁴]	Radius of gyration [cm]	Price [CHF/m]
1	76.1	4	9.06	59.1	2.55	57.4
2	76.1	5	11.2	70.9	2.52	65.9
3	88.9	4	10.7	96.3	3	70.2
4	88.9	5	13.2	116	2.97	85.1
5	88.9	6	15.6	135	2.94	90.4
6	88.9	6.3	16.3	140	2.93	95.8
7	101.6	4	12.3	146	3.45	71.8
8	101.6	5	15.2	177	3.42	88.4
9	101.6	6	18	207	3.39	98.9
10	101.6	6.3	18.9	215	3.38	111
11	101.6	8	23.5	260	3.32	137.5
12	101.6	10	28.8	305	3.26	177
13	114.3	4	13.9	211	3.90	81.8
14	114.3	5	17.2	257	3.87	102
15	114.3	6	20.4	300	3.83	114
16	114.3	6.3	21.4	313	3.82	125.5
17	114.3	8	26.7	379	3.77	158.5
18	114.3	10	32.8	450	3.70	201
19	139.7	4	17.1	393	4.80	119.5
20	139.7	5	21.2	481	4.77	125.5
21	139.7	6	25.2	564	4.73	137.5
22	139.7	6.3	26.4	589	4.72	155.5
23	139.7	8	33.1	720	4.66	191.5

24	139.7	10	40.7	862	4.60	240
25	139.7	12	48.1	990	4.53	290
26	139.7	12.5	50	1020	4.52	306
27	168.3	4	20.6	697	5.81	135
28	168.3	5	25.7	856	5.78	167
29	168.3	6	30.6	1009	5.74	198.5
30	168.3	6.3	32.1	1053	5.73	204
31	168.3	8	40.3	1297	5.67	276
32	168.3	10	49.7	1564	5.61	317
33	168.3	12	58.9	1810	5.54	357
34	168.3	12.5	61.2	1868	5.53	387
35	177.8	5	27.1	1014	6.11	208
36	177.8	6	32.4	1196	6.08	213
37	177.8	6.3	33.9	1250	6.07	233
38	177.8	8	42.7	1541	6.01	270
39	177.8	10	52.7	1862	5.94	335
40	177.8	12	62.5	2159	5.88	390
41	177.8	12.5	64.9	2230	5.86	411
42	193.7	5	29.6	1320	6.67	201.3
43	193.7	6	35.4	1560	6.64	238
44	193.7	6.3	37.1	1630	6.63	244
45	193.7	8	46.7	2016	6.57	307

Table A.2 Cable properties

N°	Diameter [mm]	Cross-section [mm ²]	Maximum axial force [kN]	Price [CHF/m]
1	6	28.27	31.8	6.10
2	7	38.48	43.3	7.30
3	8	50.26	56.5	8.80
4	9	63.62	71.5	10.20
5	10	78.54	88.4	10.80
6	11	95.03	107	14.80
7	12	113.10	128	17.90
8	13	132.73	150	19.80
9	14	153.94	173	23.90
10	15	176.71	199	24.70
11	16	201.06	226	24.90
12	18	254.47	286	37
13	20	314.16	354	38.30
14	22	380.13	428	49.25
15	24	452.39	509	47.20
16	26	530.93	597	58.10
17	28	615.75	693	66.10
18	30	706.86	795	74.90
19	32	804.25	911	83.20
20	34	907.92	1030	106.45
21	36	1017.88	1153	110.30
22	40	1256.64	1424	133.20

References

- [1] Motro R. Tensegrity: Structural Systems for the Future. Hermes ed. UK: Penton Science 2003.
- [2] Skelton RE, de Oliveira MC. Tensegrity systems: Springer 2009.
- [3] Wang BB, Li YY. Novel cable-strut grids made of prisms: I. Basic theory and design. *Journal of the International Association for Shell and Spatial Structures*. 2003;44(2):93-108.
- [4] Wang BB. Free-Standing Tension Structures From Tensegrity Systems to Cable-Strut Systems Routledge, UK 2004.
- [5] Paronesso A, Passera R. The cloud of Yverdon. IASS Symposium 2004. 2004:184-5.
- [6] Paronesso A. The 2002 World Cycling Center Arena Aigle, Switzerland. *International IASS Symposium on "Lightweight Structures in Civil Engineering"*. Warsaw, Poland 2002.
- [7] Klimke H, Stephan S. The making of a tensegrity tower. *IASS 2004 Symposium, International Association for Shell and Spatial Structures*. Montpellier: Editions de l'Espérou 2004.
- [8] Schlaich M. The messeturm in Rostock - A tensegrity tower. *Journal of The International Association for Shell and Spatial Structures*. 2004;45(145):93-8.
- [9] Fest E, Shea K, Smith IFC. Active Tensegrity Structure. *Journal of Structural Engineering*. 2004;130(10):1454-65.
- [10] Adam B, Smith IFC. Self-Diagnosis and Self-Repair of an Active Tensegrity Structure. *Journal of Structural Engineering*. 2007;133(12):1752-61.
- [11] Adam B, Smith IFC. Reinforcement Learning for Structural Control. *Journal of Computing in Civil Engineering*. 2008;22(2):133-9.
- [12] Bel Hadj Ali N, Smith IFC. Dynamic behavior and vibration control of a tensegrity structure. *International Journal of Solids and Structures*. 2010;47(9):1285-96.
- [13] Motro R, Raducanu V. Tensegrity Systems. *International Journal of Space Structures*. 2003;18:77-84.
- [14] Motro R. Tensegrity systems: the state of the art. *International Journal of Space Structures*. 1992;7(2):75-82.
- [15] Hanaor A. Aspects of Design of Double-Layer Tensegrity Domes. *International Journal of Space Structures*. 1992;7:101-13.
- [16] Quirant J, Kazi-Aoual MN, Motro R. Designing tensegrity systems: the case of a double layer grid. *Engineering Structures*. 2003;25(9):1121-30.
- [17] Abedi K, Shekastehband B. Static Stability Behaviour of Plane Double-Layer Tensegrity Structures. *International Journal of Space Structures*. 2008;23:89-102.
- [18] Micheletti A. Una Passerella Tensintegra nel Campus di TorVergata. *FORUM Universita` Lavoro, Archiday*. Rome, TorVergata University 2009.
- [19] Micheletti A. Modular Tensegrity Structures: The TorVergata Footbridge. *Proceedings of the Colloquium Lagrangianum, Montpellier, France* 2003.
- [20] Wang BB, Li YY. From tensegrity grids to cable-strut grids. *International Journal of Space Structures*. 2001;16(4):279-314.
- [21] Wang BB, Li YY. Novel cable-strut grids made of prisms: II. Deployable and architectural studies. *Journal of the International Association for Shell and Spatial Structures*. 2003;44(2):109-25.
- [22] Jensen O, Wroldsen AS, Lader PF, Fredheim A, Heide M. Finite element analysis of tensegrity structures in offshore aquaculture installations. *Aquacultural Engineering*. 2007;36(3):272-84.

- [23] Liapi KA. Tensegrity structures for the Hellenic Maritime Museum. *IASS Symposium: Evolution and Trends in Design, Analysis and Construction of Shell and Spatial Structures*. Valencia 2009:2233-42.
- [24] de Oliveira MC, Skelton RE, Waileung C. Minimum Mass Design of Tensegrity Towers and Plates. *Decision and Control, 2006 45th IEEE Conference on* 2006:2314-9.
- [25] Motro R, Maurin B, Silvestri C. Tensegrity Rings and the Hollow Rope. *IASS Symposium 2006, New Olympics, New Shells and Spatial Structures*. Beijing 2006:470-1.
- [26] Rhode-Barbarigos L, Jain H, Kripakaran P, Smith IFC. Design of tensegrity structures using parametric analysis and stochastic search. *Engineering with Computers*. 2010;26(2):193-203.
- [27] Rhode-Barbarigos L, Bel Hadj Ali N, Motro R, Smith IFC. Designing tensegrity modules for pedestrian bridges. *Engineering Structures*. 2010;32(4):1158-67.
- [28] Kebiche K, Kazi-Aoual MN, Motro R. Geometrical non-linear analysis of tensegrity systems. *Engineering Structures*. 1999;21(9):864-76.
- [29] Masic M, Skelton RE, Gill PE. Optimization of tensegrity structures. *International Journal of Solids and Structures*. 2006;43(16):4687-703.
- [30] Bel Hadj Ali N, Sellami M, Cutting-Decelle A-F, Mangin J-C. Multi-stage production cost optimization of semi-rigid steel frames using genetic algorithms. *Engineering Structures*. 2009;31(11):2766-78.
- [31] Hojjat A, Kamal CS. *Cost Optimization of Structures*. England: John Wiley & Sons 2006.
- [32] Saidani M, Remise E. Light-weight self-stressed systems or tensegrity. *Journal of the International Association for Shell and Spatial Structures*. 2002;43(140):179-85.
- [33] Pellegrino S. *Mechanics of kinematically indeterminate structures*. PhD Thesis, University of Cambridge, U.K., 1986.
- [34] Barnes MR. Form Finding and Analysis of Tension Structures by Dynamic Relaxation. *International Journal of Space Structures*. 1999;14:89-104.
- [35] Vassart N, Motro R. Multiparametered Formfinding Method: Application to Tensegrity Systems. *International Journal of Space Structures*. 1999;14:147-54.
- [36] Paul C, Lipson H, Cuevas FV. Evolutionary form-finding of tensegrity structures. *Genetic and Evolutionary Computation Conference*. Washington D.C. 2005:3-10.
- [37] Tibert AG, Pellegrino S. Review of Form-Finding Methods for Tensegrity Structures. *International Journal of Space Structures*. 2003;18:209-23.
- [38] Juan SH, Mirats Tur JM. Tensegrity frameworks: Static analysis review. *Mechanism and Machine Theory*. 2008;43(7):859-81.
- [39] Motro R. *Tensegrity: Structural systems for the future*. Hermes ed. U.K. 2003.
- [40] Calladine CR. Buckminster Fuller's tensegrity structures and Clerk maxwell's rules for the construction of stiff frames. *International Journal of Solids and Structures*. 1978;14(2):161-72.
- [41] Pellegrino S. Structural computations with the singular value decomposition of the equilibrium matrix. *International Journal of Solids and Structures*. 1993;30(21):3025-35.
- [42] Schenk M, Guest SD, Herder JL. Zero stiffness tensegrity structures. *International Journal of Solids and Structures*. 2007;44(20):6569-83.
- [43] Day AS. An introduction to dynamic relaxation. *The Engineer*. 1965;219:218-21.
- [44] Murakami H. Static and dynamic analyses of tensegrity structures. Part 1. Nonlinear equations of motion. *International Journal of Solids and Structures*. 2001;38(20):3599-613.
- [45] Masic M, Skelton RE, Gill PE. Algebraic tensegrity form-finding. *International Journal of Solids and Structures*. 2005;42(16-17):4833-58.
- [46] Guest S. The stiffness of prestressed frameworks: A unifying approach. *International Journal of Solids and Structures*. 2006;43(3-4):842-54.

- [47] International Federation of Structural Concrete: Guidelines for the design of footbridges. fib-bulletin, 32. Novembre 2005.
- [48] Schlaich M. Planning conditions for footbridges. *Footbridges 2002 - Design and dynamic behaviour of footbridges*. Paris, November 20-22, 2002:40-52.
- [49] Butz C. Codes of practice for lively footbridges: state of the art and required measures. *Footbridges 2008 - Footbridges for urban renewal*. Porto, July 2-4, 2008:51-67.
- [50] Design Manual for Roads and Bridges: Design Criteria for Footbridges: BD 29/04, Highway agency, London, February, 2004
- [51] SIA 261 - Actions on Structures: Swiss Society of Engineers and Architects, Zurich, 2003.
- [52] SIA 260 - Basis of Structural Design: Swiss Society of Engineers and Architects, Zurich, 2003.
- [53] SIA 263 - Steel Construction: Swiss Society of Engineers and Architects, Zurich, 2003.

This work is licensed under a Creative Commons Attribution-NonCommercial-NoDerivatives 4.0 International License

